Available online at www.sciencedirect.com
SCIENCE DIRECT®
Journal of Human Evolution 46 (2004) 719–738

Convergence of forelimb and hindlimb Natural Pendular Period in baboons (*Papio cynocephalus*) and its implication for the evolution of primate quadrupedalism

D.A. Raichlen*

Department of Anthropology, The University of Texas at Austin, 1 University Station C3200, Austin, TX 78712, USA

Received 1 September 2003; accepted 1 April 2004

Abstract

The patterns of muscle mass distribution along the lengths of limbs may have important effects on the mechanics and energetics of quadrupedalism. Specifically, Myers and Steudel (J. Morphol. 234 (1997) 183) have shown that fore- and hindlimb Natural Pendular Periods (NPPs) may affect quadrupedal kinematics and must converge to reduce locomotor energetic costs. This study quantifies patterns of limb mass distribution in a live sample of *Papio cynocephalus* using limb inertial properties (mass, center of mass, mass moment of inertia, and radius of gyration). These inertial properties are calculated using a geometric modeling technique similar to that of Crompton et al. (Am. J. phys. Anthrop. 99 (1996) 547). The inertial properties in *Papio* are compared to those of *Canis* from Myers and Steudel (J. Morphol. 234 (1997) 183).

The *Papio* sample has convergent fore- and hindlimb NPPs. Additionally, these limb NPPs are relatively large compared to those of *Canis* due to the relatively distally distributed limb mass in the *Papio* sample (relatively large limb masses, relatively distal centers of mass and radii of gyration, and relatively large limb mass moments of inertia). This relatively distal limb mass appears related to the grasping abilities of their hands and feet.

Causal links are explored between limb shape adaptations for grasping hands and feet and the kinematics of primate quadrupedalism. In particular, if primates in general follow *Papio*'s limb mass distribution pattern, then relatively large limb NPPs may lead to the relatively low stride frequencies already documented for primates. The kinematics of primate quadrupedalism appears to have been strongly influenced by both selection for grasping hands and feet and selection for reduced locomotor energetic costs.

Keywords: Inertial properties; Quadrupedalism; Natural pendular period; Biomechanics

Introduction

Primates have well-developed grasping abilities in their hands and feet (Cartmill, 1972, 1992; Lemelin, 1999; Hamrick, 2001). This adaptation is

* Corresponding author
E-mail address: draichlen@mail.utexas.edu (D.A. Raichlen).

0047-2484/04/$ - see front matter © 2004 Elsevier Ltd. All rights reserved.
doi:10.1016/j.jhevol.2004.04.002

considered a hallmark of the primate order and is thought by many to have been instrumental in the origins of primates (Cartmill, 1972, 1992; Lemelin, 1999; Hamrick, 2001). Although the effects of grasping abilities on the bony morphology of the limbs have been examined in depth (e.g. Lemelin and Grafton, 1998; Lemelin, 1999; Hamrick et al., 1999; Hamrick, 2001), the effects of prehensile hands and feet on primate soft tissue have received less attention.

In general, research into primate musculature has focused on how relative differences in individual muscle masses relate to differences in substrate use or locomotor behavior (e.g. Fleagle, 1977; Grand, 1977). Very few researchers have focused on a detailed analysis of muscle mass distribution using limb inertial properties (mass, center of mass, mass moment of inertia, and radius of gyration), which provide quantitative data describing overall limb shape (see Reynolds, 1974; Vilensky, 1979; Wells and DeMenthon, 1987). Although understanding variation among individual muscle masses is essential when examining differences in locomotor behaviors, the *distribution* of this muscle mass on the limbs may have important effects on locomotor capacity, both in terms of energetics (Steudel, 1990; Hildebrand and Hurley, 1985) and on an organism's ability to accelerate (Preuschoft and Gunther, 1994).

Selection for grasping abilities in the hands and feet has produced primate limbs that appear to have relatively large concentrations of distal muscle mass for their size (Grand, 1977; Alexander et al., 1981; Preuschoft and Gunther, 1994). Grand (1977) determined that quadrupedal primates have a greater proportion of body mass located in their forearms, hands, lower legs, and feet than in their upper limb segments (arms and thighs) when compared to *Canis*. Finger and toe flexors along with wrist and ankle deviators constitute the majority of this mass (Grand, 1977). By contrast, the distal limb segment masses of *Canis* are comprised primarily of bone (Grand, 1977). Others have alluded to these differences in limb mass distribution between primates and non-primate mammals (Preuschoft and Gunther, 1994; Larson, 1998), but there is a paucity of primate inertial property data available to interpret these differences within a biomechanical context.

This study examines limb inertial properties in a sample of *Papio cynocephalus* to determine how selection for grasping hands and feet has affected limb inertial properties. Additionally, the implications of limb mass distribution patterns on the mechanics of quadrupedalism are examined. Finally, since the mechanics of quadrupedalism are related to energy saving mechanisms (see Hildebrand, 1985), the effects of limb mass distribution are examined in light of these known energy saving mechanisms.

An important energy saving characteristic of walking in quadrupeds is the pendular exchange of potential and kinetic energy throughout a step cycle (Hildebrand, 1985). During swing phase, if the limb swings as a pure pendulum, muscular activity is needed only to raise the limb off the ground (peak potential energy) and to decelerate the limb at the end of swing phase. Gravity and inertial forces convert potential energy into kinetic energy as the limb swings in the direction of progression. Therefore, swinging the limbs as pure pendula reduces locomotor costs (Hildebrand, 1985).

If a limb swings with a maximal exchange of kinetic and potential energy (and therefore minimal energy expenditure), the time it takes to complete one full oscillation is referred to as the Natural Pendular Period (NPP) of the limb. When a limb swings as a physical pendulum, its NPP is determined by both its length, and the distribution of mass along its length. Longer limbs, as well as limbs with more distally distributed mass, generally have larger NPPs (see Myers and Steudel, 1997).

Limb NPP may therefore be an important morphological correlate of locomotor kinematics in quadrupeds. There have been suggestions, though, that limb motion during swing phase is not passive, but is driven by muscular action (see Jungers and Stern, 1983; Whittlesey et al., 2000). Whittlesey et al. (2000) provides a convincing case for the non-passive nature of swing phase based on the inability of pure pendular motion to completely predict the kinematics and kinetics of human swing phase (see also Selles et al., 2001). Additionally,

muscles acting on the shoulder and hip are active during swing phase in both humans and quadrupeds, although this activity is concentrated mostly at the beginning and the end of swing phase (see Basmajian, 1978; English, 1978a,b; Goslow et al., 1981; Larson and Stern, 1989; Whitehead and Larson, 1994).

Although the limbs of terrestrial mammals do not appear to swing without muscular action, there is strong evidence that the swing periods of humans and quadrupeds approximate their limb NPPs (Mochon and McMahon, 1980; Hildebrand, 1985; Turvey et al., 1988; Holt et al., 1990). Additionally, increasing limb NPP by loading distal limb elements in both humans and quadrupeds significantly increases stride durations and swing durations (Inman et al., 1981; Martin, 1985; Holt et al., 1990; Skinner and Barrack, 1990; Steudel, 1990; Mattes et al., 2000). Therefore, despite the evidence that swing phase during walking may not be achieved by a purely passive pendular mechanism, limb NPPs may be used as qualitative predictor of swing phase mechanics. That is, larger NPPs should be associated with longer swing phase durations, although the actual swing times may not be equivalent to those predicted from limb NPPs.

Forelimb and hindlimb NPP convergence as an energy-saving mechanism

Myers and Steudel (1997) argued that all four limbs of a quadruped should have equivalent NPPs. Their argument was based on two important lines of evidence. First, experimental evidence has shown that all four limbs in quadrupeds have similar swing durations during locomotion (Arshavski et al., 1965; Alexander and Jayes, 1983; Biewener, 1983; Vilensky et al., 1988). Second, Hildebrand (1985) noted that there is an energetic cost associated with swinging a limb at a period other than its NPP. Furthermore, Rosenblum and Turvey (1988) found that limbs swinging at periods other than their NPPs have more erratic swings with fluctuations in amplitude and duration. There is a cost, both energetic and rhythmic, associated with swing phase deviations from limb NPP. So, if all four limbs have similar swing phase durations, then all four limbs should have similar NPPs in order to reduce locomotor costs (Myers and Steudel, 1997).

By measuring limb inertial properties, Myers and Steudel (1997) found that in canids, and possibly other mammals in general, fore- and hindlimb NPPs do in fact converge. The results from their study show that a quadruped can have convergent fore- and hindlimb NPPs despite differences in limb lengths (Myers and Steudel, 1997). Canids achieve NPP convergence due to the fact that their shorter forelimbs carry mass more distally compared to their hindlimbs (Myers and Steudel, 1997). Myers and Steudel (1997) extended their findings from *Canis* to quadrupedal mammals in general given that, across large ranges of body size, mammals are geometrically similar in shape.

Two primates were included in Myers and Steudel's (1997) study. *Lemur fulvus* (data from Wells and DeMenthon, 1987) has convergent fore- and hindlimb NPPs (Myers and Steudel, 1997). However, Myers and Steudel (1997) found that in *Macaca mulatta*, fore- and hindlimb NPPs differ by approximately 7% (*Macaca mulatta* data from Vilensky, 1979). Since selection pressures on primates have included the need for grasping extremities as well as reduced locomotor energy expenditure, it is possible that these competing selection pressures may explain the difference in limb NPPs found in rhesus macaques. Perhaps selection for grasping abilities differs between the fore- and hindlimbs of some primates, causing NPPs to differ as well. Differences between fore- and hindlimb NPPs among primates in general seem unlikely because any divergences imply increases in locomotor energetic costs (see Hildebrand, 1985). Any differences would conflict with studies showing quadrupedal primates, with the exception of chimpanzees, to have similar locomotor energetic costs compared to other quadrupedal mammals (Taylor et al., 1982; Heglund, 1985; Steudel-Numbers, 2003).

The goal of this study was to test whether *Papio cynocephalus* exhibits divergent fore- and hindlimb NPPs. Despite the limb shape differences between primate and non-primate mammalian quadrupeds, *Papio* is hypothesized here to have convergent fore- and hindlimb NPPs in order to maintain low energetic costs of locomotion.

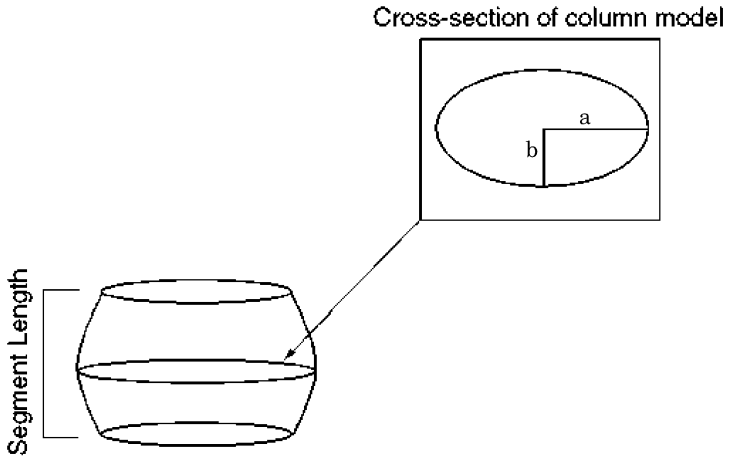

Fig. 1. Elliptical column model (after Crompton et al., 1996). Inset is a cross-section of the column where a and b are the lengths of the major and minor axes respectively. In this model, the lengths a and b vary independently with the length of the column. The values for a and b must be taken at three positions along the length of the segment and are used to generate segment inertial properties using equations developed in Appendix A.

Methods

Geometric model

This study employs a geometric modeling technique based on one developed by Crompton et al. (1996) to determine the mass properties of limb segments. This method was used to allow collection of inertial property data from healthy, active, and live adult animals. Crompton et al. (1996) developed a geometric model that takes into account the irregularity of limb shape. Their model is based on a column with an ellipsoidal cross-section. The major and minor axes of the ellipsoids vary with each other along the length of the column by a constant, k (Crompton et al., 1996). The limb of a living animal may then be modeled by taking external measurements along the length of the limb segments (Crompton et al., 1996). The only drawback is that in their model, the major and minor axes do not vary independently.

The model used for this study is based on Cromptons et al.'s (1996) geometric model with the exception of the fact that the major and minor axes of the columns can vary independently with the length of the segment. Eq. (1) describes an elliptical cross-section (centered at the origin) where a and b describe the length of the major and minor axis of the ellipse (half the length of the longest and shortest axes of the ellipse; see Fig. 1):

$$\frac{x^2}{a^2}+\frac{y^2}{b^2}=1 \tag{1}$$

Two curves may then be used to describe the shape of the column (Fig. 1). One curve describes how the major axis (a) changes with the length of the segment. The other curve describes how the minor axis (b) changes with the length of the segment. The length of these curves is equal to the length of the segment.

The shape of the two curves described above were found by taking three measurements of major and minor axes along the length of each limb segment (arm, forearm, hand, thigh, shank, and foot), as well as one measure of the length of the segment (see *Measurements protocols and sample*).

For each segment, the lengths of the major and minor axes were plotted against the measurement position (distance from the proximal end of the segment to the measurement position) and second order polynomials were fit to those data. The inertial properties (mass, center of mass, mass moment of inertia) for these segments were then calculated using equations developed in Appendix A.

Calculating the NPP

Once the inertial properties of all limb segments are calculated, the limb NPP may be calculated assuming the limb acts as a physical pendulum (Myers and Steudel, 1997):

$$NPP=2\pi\sqrt{\frac{I}{Mg(CM)}} \quad (2)$$

In Eq. (2), I is the limb's mass moment of inertia about the proximal joint (the shoulder in the forelimb or the hip in the hindlimb), M is the limb's mass, g is acceleration due to gravitational forces (9.8 m/s^2), and CM is the distance of the center of mass from the proximal joint.

The calculation of the center of mass of a limb can be found using the following equation (from Tipler, 1976):

$$CM=\frac{\sum_{i=1}^{n} m_i r_i}{\sum_{i=1}^{n} m_i} \quad (3)$$

Where m_i is the mass of the ith segment, and r_i is the distance of the center of mass of the ith segment from the proximal end of the limb. The denominator is the calculation for the total mass of the limb (M). The mass moment of inertia describes a body's resistance to angular acceleration and can be found using the following equations:

$$I_{cm}=\sum_{i=1}^{n} m_i r_i^2+I_i \quad (4)$$

$$I_p=I_{cm}+M(CM^2) \quad (5)$$

Where I_{cm} is the whole limb mass moment of inertia about its CM, I_i is the ith's segment mass moment of inertia about its CM, and I_p is the whole limb mass moment of inertia about a transverse axis through the proximal end of the segment (i.e. the resistance of the limb to angular acceleration during swing phase). Finally, the limb radius of gyration (RG) about the proximal end can be found using the equation (from Myers and Steudel, 1997):

$$RG=\sqrt{\frac{I_p}{M}} \quad (6)$$

This variable is an important measure of overall limb mass distribution as it is the position on a body where a point mass would have an equal mass moment of inertia to the body itself. From Eqs. (3)–(6), it should be apparent that if limbs carry relatively distal mass, the CM and RG positions will be relatively distal and the mass moment of inertia will be relatively large.

Measurement protocols and sample

Measurements were taken on live adult baboons (*Papio cynocephalus*; n=9). This sample size is comparable to samples in similar studies of primate inertial properties in the literature (see Reynolds, 1974; Vilensky, 1979; Wells and DeMenthon, 1987). Baboons were measured at the Southwest Foundation for Biomedical Research in San Antonio, TX while animals were anesthetized for their annual medical exams. Body mass was measured on a scale to the nearest 0.1 kg. Animals were anesthetized using Ketamine and placed face down on a gurney with one arm and one leg hanging over the side. In this way, limb shapes during measurements best-approximated limb shape during locomotion. Segment lengths were measured using measuring tape. Major and minor axes lengths were taken using spreading calipers at the proximal, distal, and mid-segment lengths.

The following segment definitions were used to define the proximal and distal ends of the segments:

1. The upper arm was defined proximally by a point in between the acromion process of the scapula and the greater tubercle of the humerus and was defined distally by the most proximal edge of the radial head.
2. The forearm was defined proximally by the most proximal edge of the radial head and was defined distally by the styloid process of the radius.

3. The hand was defined proximally by the styloid process of the distal radius and was defined distally by the end of the longest digit.
4. The thigh was defined proximally by the greater trochanter and was defined distally by the caudal edge of the lateral condyle of the femur.
5. The shank was defined proximally by the proximal edge of the lateral tibial condyle and was defined distally by the lateral malleolus of the fibula.
6. The foot was defined proximally by the posterior edge of the calcaneous and distally by the tip of the longest digit. (Note: when computing whole limb inertial properties, the proximal edge of the foot was considered to be the position at which it attaches to the ankle. In this way, the whole limb inertial properties more closely approximate those of straightened whole limbs for comparison with data from the literature).

Validity of the model

Before a geometric model can be used in an analysis of limb shape, its validity must be determined. A comparison of predicted and measured masses and CMs of limbs and limb segments was used to assess the validity of the model. Limbs were removed from the body of one baboon cadaver and frozen in a straightened position. Limbs were also removed from the bodies of two other baboon cadavers for segmentation. An oscillating saw was used to cut each limb into discrete columns. This procedure eliminated limb flexion as well as extraneous tissue at the proximal ends of the limbs. The total sample for model testing was three whole limbs and six limb segments. The mass of each limb and limb segment was determined experimentally using a scale. The CM position of each limb and limb segment was determined by placing the segment on a tray with a known CM, and balancing the segment/tray unit on a fulcrum (see Myers and Steudel, 1997). Each limb (n=3), or limb segment (n=6), was also modeled using the geometric column model described above and compared using paired t-tests.

Data analysis

Direct comparison of limb inertial properties between *Papio* and *Canis* is not possible because these taxa do not overlap in body size. Therefore, inertial properties for each taxon were normalized by creating a set of dimensionless inertial properties. Inertial properties were made dimensionless by dividing each value by a fundamental quantity (or combination of quantities) of the same dimension that is constant in size and biologically relevant (see Hof, 1996). If inertial properties in *Canis* and *Papio* are geometrically similar, then larger body masses and longer limb lengths should be associated with larger limb inertial property values. Therefore, the use of body mass and limb length as fundamental quantities removes differences between taxon inertial properties due simply to geometric scaling.

The dimensionless set of inertial properties were constructed after Hof (1996) as follows: Limb masses (unit: kg) were divided by body mass, length variables (RG and CM; unit: m) were divided by limb length, NPPs (unit: s) were divided by $(\text{limb length}/g)^{\frac{1}{2}}$ (see Hof, 1996 for a complete derivation of the fundamental time quantity) where g is the gravitational acceleration constant (9.8 m/s^2), and mass moments of inertia (unit: $kg*m^2$) were divided by the product of body mass and the square of limb length.

Paired t-tests were used to determine whether fore- and hindlimb raw inertial properties differed significantly. The 95% confidence intervals were calculated for taxon specific means of dimensionless inertial properties to determine whether the *Papio* sample overlaps with *Canis*.

Results

Model validity

In the case of both mass and CM, the measured and predicted values do not differ significantly for the cadaver sample (Table 1). Additionally, measured and predicted masses are highly correlated (r=0.998; Fig. 2a), as are measured and predicted CMs (r=0.996; Fig. 2b). Neither regression

Table 1
Descriptive statistics for model validity

Property	Mean measured	Mean predicted	Mean % difference	Max % difference	Min % difference	Paired *t*-test significance
Mass	996.64	952.22	4.80	14.60	−0.23	ns
CM	11.98	12.30	−2.69	−9.19	0.00	ns

Note: ns refers to non-significant *p*-values at α=0.05.

line differs significantly from the line of identity ($y=x$; see figure legend). These results support the use of the model for calculating inertial properties and making comparisons of these properties with published values for other taxa.

Convergence of forelimb and hindlimb NPP

The means for fore- and hindlimb NPPs do not differ significantly (Table 2). Additionally, the average difference between fore- and hindlimb NPPs is 2.4% (maximum difference is 5.6%; see Table 3). These values are within the range of fore- and hindlimb NPP percent differences in Myers and Steudel's (1997) canid sample (Table 3). Although there are minor deviations, fore- and hindlimb NPPs in this sample of *Papio* do converge (i.e. they are statistically indistinguishable).

NPP convergence in *Papio* is achieved by having divergent fore- and hindlimb mass distribution patterns. The hindlimbs of the *Papio* sample are significantly longer, more massive, and have larger mass moments of inertia compared to the forelimbs (Table 2). *Papio*'s fore- and hindlimb CMs and RGs are not statistically different (Table 2). These results are similar to those of Myers and Steudel's (1997; see their Table 2) canid sample. In *Canis*, Myers and Steudel (1997) stressed the importance of the fore- and hindlimb equivalence of the ratio: $RG/(CM^{\frac{1}{2}})$. This ratio is determined by substituting RG into the NPP equation (see Eq. (2) and Eq. (5)). Both *Papio* and *Canis* achieve equivalence of this ratio by having identical RGs and CMs in the fore- and hindlimbs (Table 2; Myers and Steudel, 1997).

Comparison of limb shapes in primates and canids

The results from this comparative sample show both 1) the similarity in NPP convergence mechanism in the primate sample compared to *Canis*, and 2) the difference in limb shapes between the taxa. These differences in limb shapes are clear when dimensionless inertial properties are examined.

Papio's hindlimbs are relatively longer than its forelimbs (Fig. 3). This pattern resembles the fore- and hindlimb length differences found in Myers and Steudel's (1997) *Canis* sample (Fig. 3). In *Papio*, as in *Canis,* the hindlimb is relatively more massive than the forelimb (Fig. 4). *Papio*'s fore- and hindlimbs are relatively more massive than the fore- and hindlimbs of *Canis* respectively (Fig. 4). The dimensionless limb mass moments of inertia (I_{dim}) are also relatively greater in both the fore- and hindlimbs of *Papio* compared to *Canis* (Fig. 5). *Papio*'s hindlimbs have slightly larger I_{dim}'s than its forelimbs (Fig. 5).

In both *Papio* and *Canis*, CM (Fig. 6) and RG (Fig. 7) relative to limb length are greater in the forelimb compared to the hindlimb. These results confirm a similar mechanism of limb NPP convergence in *Papio* and *Canis* and further confirm the analysis of Myers and Steudel (1997). Though the forelimb is shorter and less massive than the hindlimb, its relatively more distal CM and RG create NPP convergence. *Papio* has relatively more distal CMs and RGs than the canid sample. At a given limb length, therefore, *Papio* has relatively larger amounts of limb mass concentrated distally than in the canid sample.

Papio and *Canis* achieve fore- and hindlimb NPP convergence (Table 2) despite shorter forelimbs, by having larger forelimb dimensionless

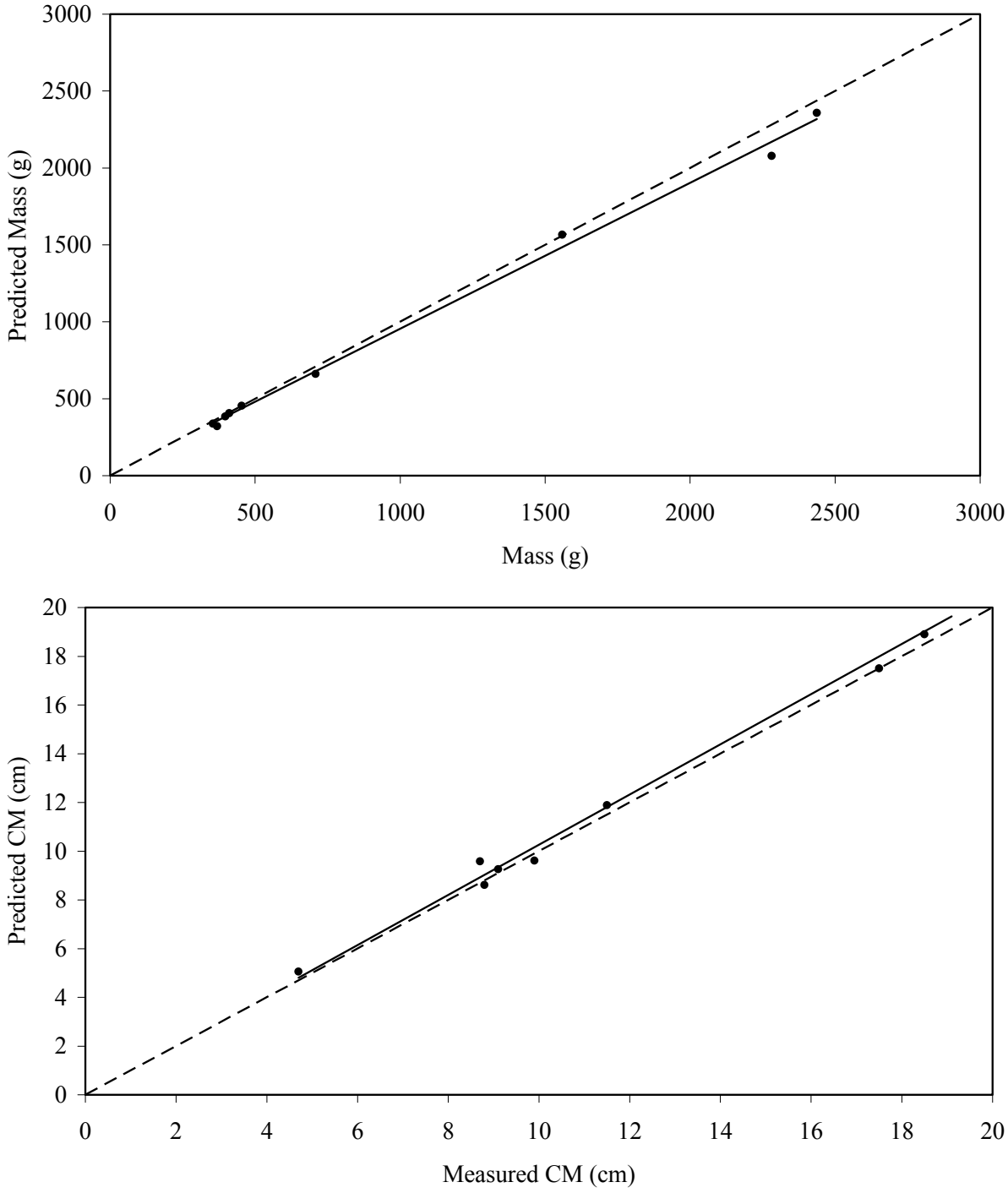

Fig. 2. (a) Predicted vs. measured mass in a sample of cadaver limbs and limb segments. The dashed line is the line of identity and the solid line is a least-squares regression (r=0.998, Slope (95% C.I.)=0.95 (0.10), Intercept (95% C.I.)=7.216 (107.034), p<0.0001). (b) Predicted vs. measured center of mass in a sample of cadaver limbs and limb segments. The dashed line is the line of identity and the solid line is a least-squares regression (r=0.996, Slope (95% C.I.)=1.03 (0.08), Intercept (95% C.I.)=0.03 (1.03), p<0.0001).

Table 2
Comparison of forelimb and hindlimb inertial properties in the primate sample

Variables	Forelimb mean	Hindlimb mean	Percent difference	Paired *t*-test significance
Limb mass (g)	1496.72	2489.04	39.87	<0.001
Limb length (cm)	59.29	68.07	12.90	<0.001
Moment of inertia (g*cm^2)	1384737.59	2331077.67	40.60	<0.001
CM (cm)	24.61	23.86	−3.14	ns
RG (cm)	30.50	30.41	−0.30	ns
NPP (s)	1.23	1.24	0.81	ns

Note: ns refers to non-significant *p*-values at α=0.05. Percent difference is the difference between hindlimb and forelimb means as a percentage of the hindlimb mean.

Table 3
Percent differences between forelimb and hindlimb NPPs in the primate and *Canis* samples

Taxa	Mean % difference (95% confidence interval)	Minimum % difference	Maximum % difference
Papio	2.35 (1.36)	0.10	5.58
Canis	1.83 (1.255)	0	7.14

Note: Percent difference is the difference between hindlimb and forelimb NPP as a percentage of hindlimb NPP.

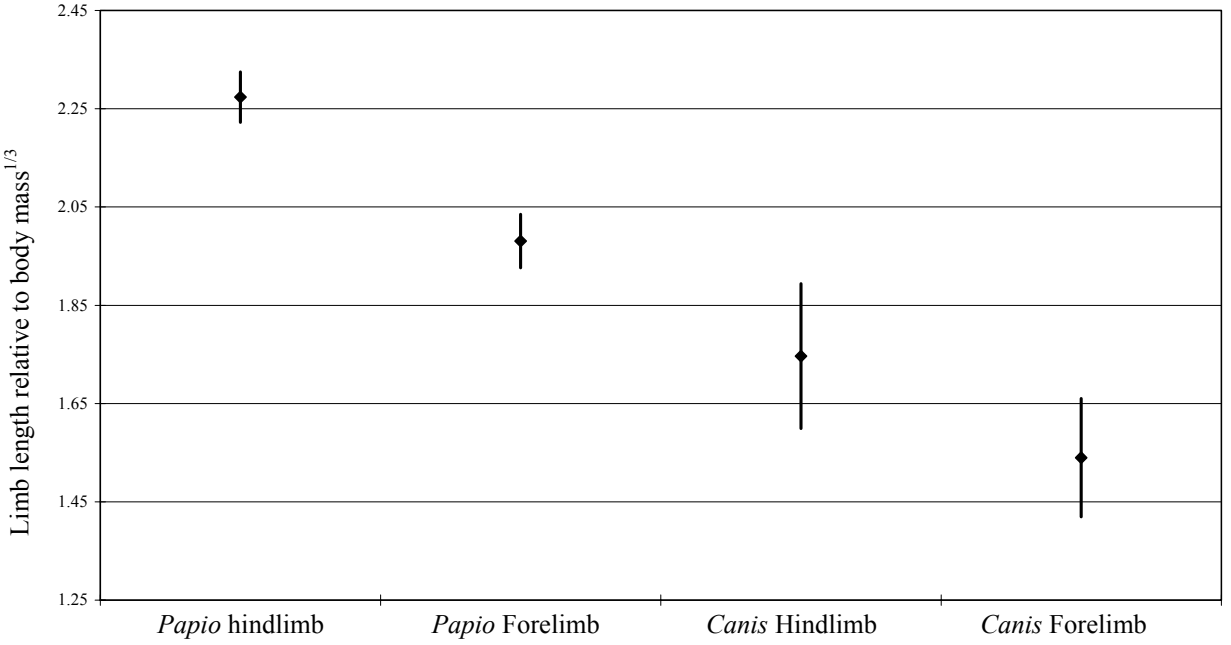

Fig. 3. Limb length relative to the cube root of body mass; diamonds are means, and lines represent the upper and lower 95% confidence intervals (see Table 4 for values of means and confidence intervals). *Canis* from Myers and Steudel (1997).

NPPs compared to their hindlimbs (Fig. 8). *Papio* has larger fore- and hindlimb dimensionless NPPs compared to the canid fore- and hindlimb dimensionless NPPs respectively. The dimensionless forelimb NPP of *Canis* overlaps with the dimensionless hindlimb NPP of *Papio*. This overlap is a

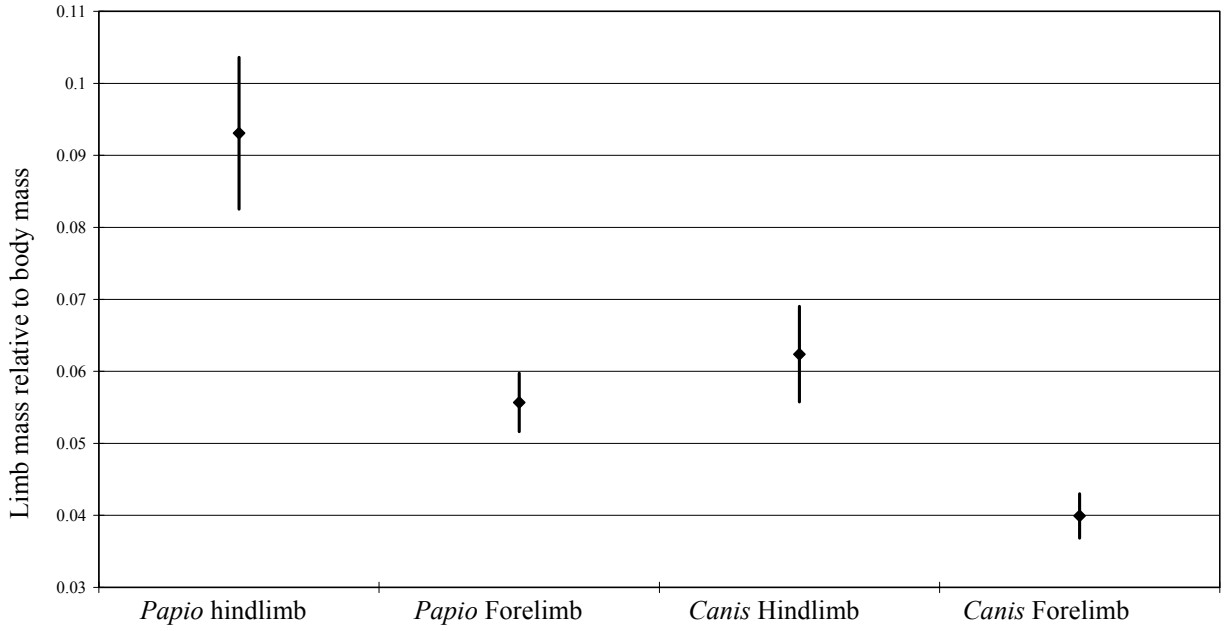

Fig. 4. Limb mass relative to body mass; diamonds are means, and lines represent the upper and lower 95% confidence intervals (see Table 4 for values of means and confidence intervals). *Canis* from Myers and Steudel (1997).

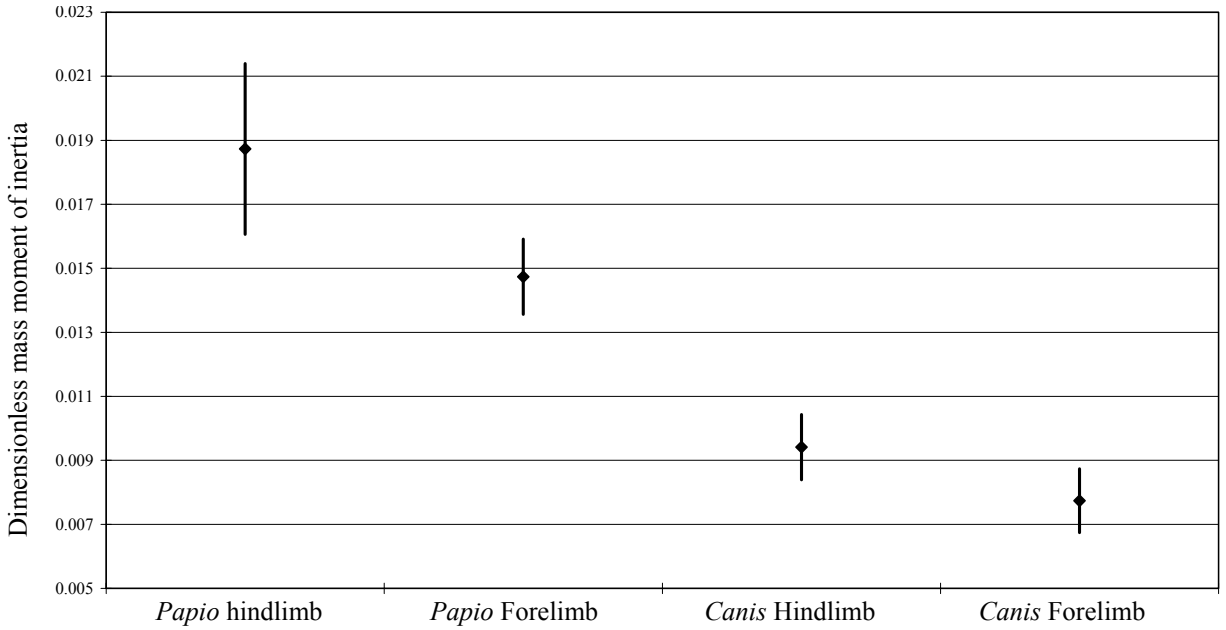

Fig. 5. Dimensionless limb mass moment of inertia; diamonds are means, and lines represent the upper and lower 95% confidence intervals (see Table 4 for values of means and confidence intervals). *Canis* from Myers and Steudel (1997).

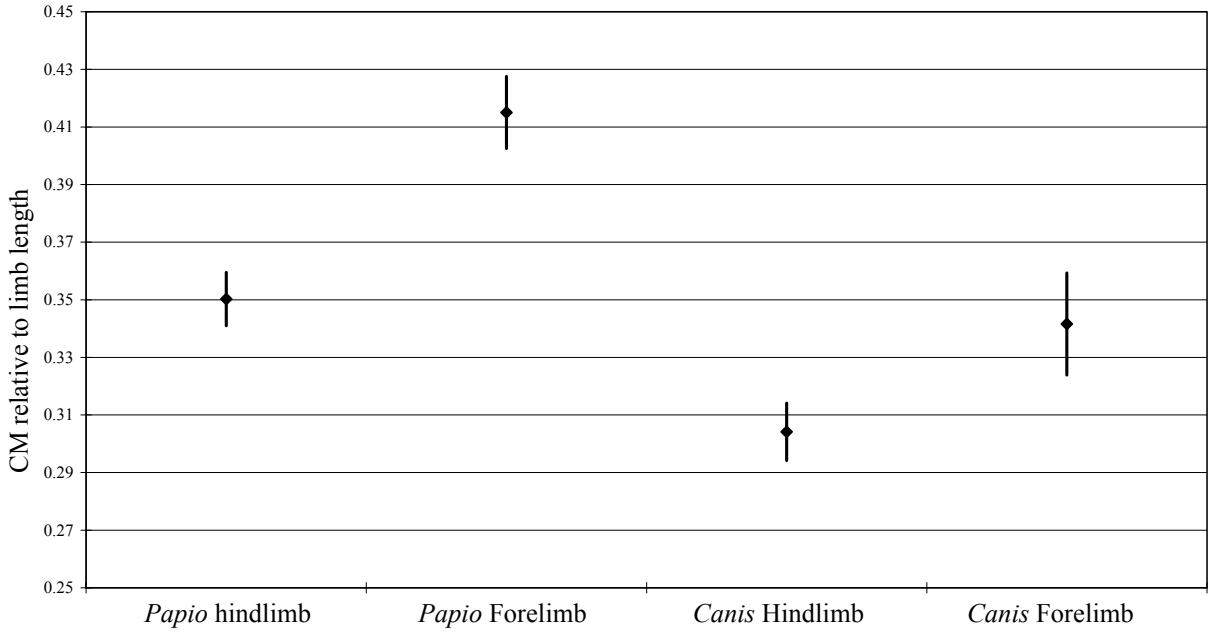

Fig. 6. CM relative to limb length; diamonds are means, and lines represent the upper and lower 95% confidence intervals (see Table 4 for values of means and confidence intervals). *Canis* from Myers and Steudel (1997).

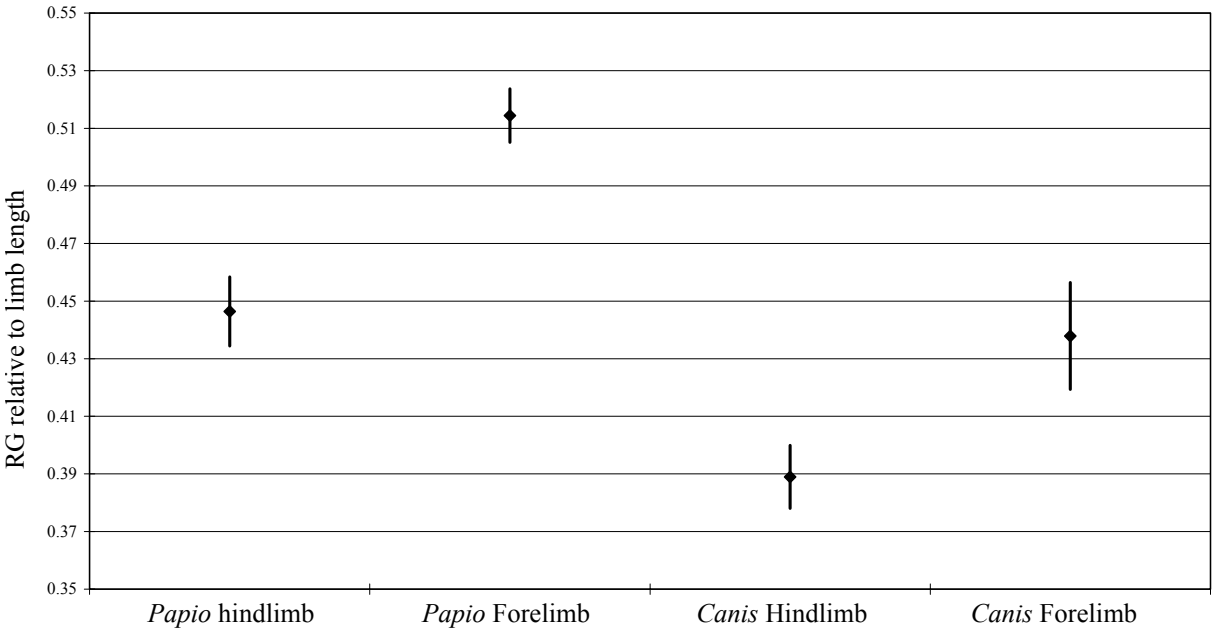

Fig. 7. RG relative to limb length; diamonds are means, and lines represent the upper and lower 95% confidence intervals (see Table 4 for values of means and confidence intervals). *Canis* from Myers and Steudel (1997).

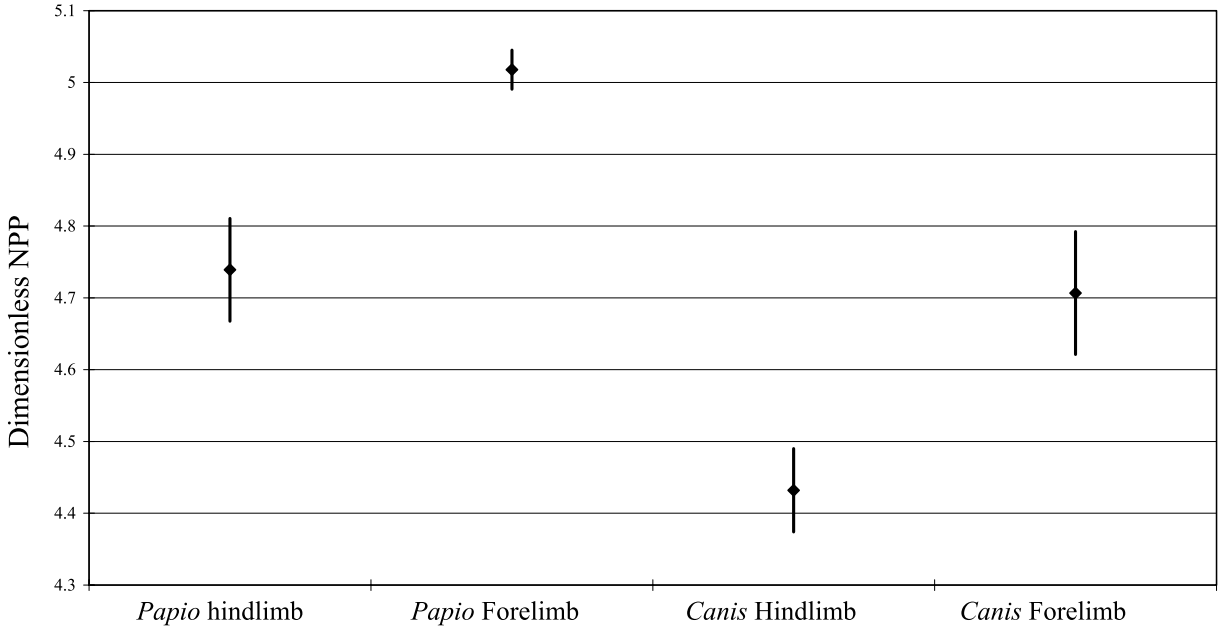

Fig. 8. Dimensionless NPP; diamonds are means, and lines represent the upper and lower 95% confidence intervals (see Table 4 for values of means and confidence intervals). *Canis* from Myers and Steudel (1997).

Table 4
Means (95% confidence intervals) for dimensionless inertial properties in *Papio* and *Canis*

Variables	*Papio* (*n*=9)	*Canis* (*n*=12)
Dimensionless hindlimb mass	0.093 (0.011)	0.062 (0.034)
Dimensionless forelimb mass	0.056 (0.004)	0.040 (0.011)
Dimensionless hindlimb length	2.105 (0.049)	1.747 (0.364)
Dimensionless forelimb length	1.963 (0.049)	1.54 (0.156)
Dimensionless hindlimb I	0.019 (0.003)	0.009 (0.004)
Dimensionless forelimb I	0.014 (0.001)	0.008 (0.001)
Dimensionless hindlimb CM	0.350 (0.009)	0.304 (0.023)
Dimensionless forelimb CM	0.420 (0.012)	0.342 (0.068)
Dimensionless hindlimb RG	0.446 (0.012)	0.389 (0.040)
Dimensionless forelimb RG	0.514 (0.009)	0.438 (0.031)
Dimensionless hindlimb NPP	4.739 (0.072)	4.432 (0.058)
Dimensionless forelimb NPP	5.018 (0.027)	4.707 (0.085)

Note: All variables made dimensionless using methods described in text. *Canis* inertial properties are taken from Myers and Steudel (1997). *I* is mass moment of inertia; CM is limb center of mass from the proximal end; RG is limb radius of gyration from the proximal end.

result of the need to have relatively large NPPs in the shorter forelimb to create convergence. Although the forelimb NPP is relatively large in *Canis*, it is still smaller than the dimensionless forelimb NPP of *Papio*).

Discussion

The baboon sample has fore- and hindlimbs that converge on the same NPP. The mechanism for fore- and hindlimb NPP convergence is very

similar in *Papio* and *Canis*. Both achieve convergence through equivalence of $RG/(CM^{\frac{1}{2}})$, and this equivalence is driven by very similar fore- and hindlimb raw CM and RG positions. In *Papio,* as in *Canis,* it is the distal mass in the forelimbs that creates NPP convergence.

Although there are minor deviations from true NPP convergence in this sample of *Papio*, none of the percent differences are larger than those of the *Canis* sample from Myers and Steudel (1997). Error inherent to the model may cause small deviations in limb NPP (see results of model accuracy). Despite any possible error, it is remarkable that fore- and hindlimb NPPs are so similar.

Impact of limb flexion on NPP

Flexion of the knee and elbow joints during swing phase will change limb NPPs by bringing distal limb elements closer to the proximal limb joint (Hildebrand, 1985; Witte et al., 1991; Preuschoft and Gunther, 1994; Myers and Steudel, 1997). In most mammals, the effects of this flexion on limb NPP appear to be minimal (Hildebrand, 1985; Myers and Steudel, 1997). In canids, for example, limb joint flexion during swing phase decreases limb NPP by only 7% (Myers and Steudel, 1997).

To examine the effects of limb joint flexion on *Papio*'s NPPs, forelimb and hindlimb NPPs for one subject from this study were calculated over a range of knee and elbow flexion angles. Because there are no swing phase kinematic data available for *Papio*, maximum swing phase knee and elbow flexion angles were estimated from figures in Vilensky and Gankiewicz (1990a); forelimb) and Vilensky and Gankiewicz (1990b); hindlimb) for vervet monkeys. Although there is clearly overlap in maximum swing phase knee and elbow flexion angles, there is some indication that in vervets, knee flexion is slightly greater than elbow flexion during swing phase. Because of this possible difference, a comparison was made of forelimb and hindlimb NPP changes given both similar angles of flexion, as well as larger knee flexion angles (Table 5).

Forelimb and hindlimb NPP convergence would not be compromised by swing phase limb joint flexion, even if the knee flexes to a greater extent than the elbow. At the same knee and elbow flexion angles, the difference between forelimb and hindlimb NPPs as a percent of hindlimb NPP does not rise higher than 2%. If the knee is flexed ten degrees greater than the elbow, the difference between forelimb and hindlimb NPP as a percent of hindlimb NPP again remains below 2%.

Estimated maximum limb flexion during swing phase reduces limb NPPs by nearly 12% in this individual (Table 5). This value is larger than the 7% reduction calculated by Myers and Steudel (1997). Dimensionless limb NPPs at maximum flexion are, however, still higher in *Papio* compared to *Canis* at its maximum limb joint flexion (*Canis* forelimb dimensionless NPP=4.22; *Canis* hindlimb dimensionless NPP=3.93; values are based on a 7% reduction in limb NPP for dog 1 reported by Myers and Steudel, 1997).

Limb mass distribution in primate quadrupeds

This is the first study to directly compare all whole limb inertial properties in a sample of quadrupedal primates and non-primates, allowing a more complete description of the possible impacts of limb mass distribution on mammals with differing limb selection pressures. The results from this study indicate that *Papio* has more distal limb mass concentrations than canids. *Papio* is considered to be a mostly terrestrial primate taxon (Fleagle, 1988) and it is therefore important to note that distally distributed limb mass that has been described for other, more arboreal primates (see Grand, 1977; Vilensky, 1979; Preuschoft and Gunther, 1994) is maintained in a more terrestrial primate quadruped.

Preuschoft and Gunther (1994) noted that *Ateles* has more distal concentrations of limb mass than *Macaca*, implying that there is some distinction between segment mass distributions in more suspensory (*Ateles*) compared to more quadrupedal (*Macaca*) primates. Although comparable inertial property data are not available in the literature for primate quadrupeds that differ in their substrate use, it is useful to compare the relative segment masses in this *Papio* sample to other, more arboreal primate quadrupeds. Table 6

Table 5
Effects of elbow and knee flexion on limb NPP in one individual *Papio*

Angles[a]	Forelimb NPP	Hindlimb NPP	Percent difference same angle[b]	Percent difference different angle[c]	Forelimb percent difference from straight	Hindlimb percent difference from straight	Forelimb dimensionless NPP	Hindlimb dimensionless NPP
180	1.24	1.23	−0.71	−0.84	0	0	5.06	4.72
170	1.24	1.23	−0.70	−1.06	0.14	0.12	5.06	4.72
160	1.23	1.23	−0.64	−1.25	0.55	0.48	5.03	4.70
150	1.22	1.22	−0.55	−1.40	1.24	1.08	5.00	4.67
140	1.21	1.21	−0.42	−1.49	2.19	1.90	4.95	4.63
130	1.20	1.20	−0.24	−1.52	3.39	2.94	4.89	4.58
120	1.18	1.18	0	−1.47	4.84	4.16	4.82	4.53
110	1.16	1.16	0.31	−1.30	6.50	5.55	4.73	4.46
100	1.14	1.14	0.70	−0.97	8.35	7.05	4.64	4.39
90	1.11	1.13	1.21	−0.42	10.34	8.59	4.54	4.32
80	1.09	1.11	1.86		12.37	10.07	4.44	4.25

[a]Flexion angles for the elbow and knee where 180 degrees is a fully extended joint.
[b]Difference between hindlimb and forelimb NPP when the elbow and knee are flexed at the same angle as a percentage of hindlimb NPP.
[c]Difference between hindlimb and forelimb NPP when the knee is flexed ten degrees more than the elbow as a percentage of hindlimb NPP.

Table 6
Mean segment masses as a percentage of total limb mass (95% confidence intervals of the mean) in three primate quadrupeds

	Papio cynocephalus n=9	*Macaca*[c] n=8	*Alouatta caraya* n=7
Arm mass	57.43 (1.61)	50.64 (2.14)	40.33 (1.37)
Below elbow mass[a]	42.57 (1.61)	49.36 (2.14)	59.67 (1.37)
Thigh mass	71.25 (2.55)	65.38 (2.49)	48.22 (2.63)
Below knee mass[b]	28.75 (2.55)	34.62 (2.49)	51.78 (2.63)

Note: data from *Macaca* and *Alouatta caraya* are from Grand (1977).
[a]Below elbow mass is the sum of the forearm and hand masses
[b]Below knee mass is the sum of the leg and foot masses
[c]Mean from 5 individuals of *M. fuscata*, and a single individual each of *M. nemestrina*, *M. nigra*, and *M. leucophaeus*.

provides the mean masses of the proximal limb segments (arm/thigh) and the means of the combined masses of limb segments below the elbow and knee as a percentage of total limb mass in three primate taxa that differ in their use of arboreal substrates (non-*Papio* data from Grand, 1977).

The most terrestrial primate in this sample (*Papio*) has the lightest distal limb segments. *Alouatta* is the most arboreal of these taxa (Fleagle, 1988), and has the heaviest distal limb segments. *Macaca* falls into a mixed terrestrial/arboreal locomotor group (Fleagle, 1988) and has distal limb segments intermediate in their relative masses compared to *Papio* and *Alouatta*.

As Preuschoft and Gunther (1994) noted, limb inertial properties may distinguish primates based on the amount of time they spend moving on arboreal substrates. It can be concluded that relatively large distal limb mass concentrations are an essential adaptation to arboreal locomotion, since these substrates presumably require the use of grasping extremities to a greater extent than during terrestrial locomotion. Additionally, the results from this study indicate that distal limb mass concentrations are maintained, although to a lesser degree, in the evolution of a more terrestrial locomotor repertoire.

Impacts of limb shape on terrestrial quadrupedalism

The distal limb mass concentrations of *Papio* lead to relatively large limb NPPs compared to the canid sample. Large NPPs should lead to increased swing durations (swing duration should approximate one half of limb NPP), which in turn increase stride duration at a given speed and reduce stride frequency (Preuschoft and Gunther, 1994; Myers and Steudel, 1997). Experimental results confirm this inverse relationship between limb NPP and stride frequency. Steudel (1990) found that the addition of weights to distal limb segments of dogs (increasing limb NPPs) resulted in significant decreases in stride frequency. These results have been confirmed in studies of limb loaded bipedal walking in humans (Inman et al., 1981; Martin, 1985; Holt et al., 1990; Skinner and Barrack, 1990; Steudel, 1990; Mattes et al., 2000). The results from this study may therefore offer a morphological cause for the low stride frequencies of primates reported by Alexander and Maloiy (1984) and Demes et al. (1990).

The implications of these results extend beyond low stride frequencies in quadrupeds with relatively large limb NPPs, since low stride frequencies are related to other gait characteristics. Among other unique kinematic and kinetic characteristics, primates have been shown to use relatively long strides as well as the low stride frequencies discussed above (Alexander and Maloiy, 1984; Reynolds, 1987; Demes et al., 1990). These two characteristics are related because velocity is the product of stride frequency and stride length. So, at a given velocity, a primate walking with relatively low stride frequencies would also walk with relatively long stride lengths. Related to these long stride lengths, primate fore- and hindlimbs undergo a larger amount of angular excursion than non-primate mammals (Larson et al., 2000,

2001). Larson et al. (2000, 2001) concluded that in order to walk with relatively long stride lengths, primates must use large fore- and hindlimb angular excursions.

Explanations for these uniquely primate characteristics have centered on their original invasion of the small branch niche proposed by Cartmill (1972). Subsequently, many have speculated that these characteristics aid primates when using arboreal quadrupedalism (see Larson et al., 2000; Larson et al., 2001). Demes et al. (1990) hypothesized that lower stride frequencies and the resultant long stride lengths at a given speed may function to avoid branch sway during arboreal quadrupedalism in some primates. The data from this study suggest a complementary argument for why primates use low stride frequencies and long stride lengths even while walking terrestrially (see Alexander and Maloiy, 1984 for a sample of primates walking terrestrially with low stride frequencies and long stride lengths). A connection between distal limb mass and kinematics does not contradict the conclusion that these features of gait evolved in a small branch arboreal habitat (grasping extremities would have been heavily selected for in this niche), but it suggests that these kinematic characteristics may persist in primates that no longer occupy this niche due to the persistence of grasping hands and feet.

The connection between limb mass distribution and some unique aspects of primate kinematics may also provide an explanation for kinematic differences on arboreal vs. terrestrial substrates. Schmitt (2003) found that a sample of primate quadrupeds increased forelimb protraction at touchdown on arboreal compared to terrestrial substrates. If limb NPPs are related to limb angular excursion, then this result is not surprising since knee and elbow flexion during swing phase may be reduced on branches. Indeed, Schmitt et al. (1994) reported that primates allow their hands to pass alongside the substrate during swing phase, indicating perhaps a more extended elbow. As noted above, a more extended elbow during swing phase results in a slightly larger forelimb NPP.

In addition to relatively large NPPs at a given body mass, the dimensionless inertial properties describe another consequence of distal limb musculature. Limb mass moments of inertia are relatively larger in the *Papio* sample compared to the canid sample. The larger mass moments of inertia imply greater resistance to angular acceleration (Tipler, 1976). As suggested by Preuschoft and Gunther (1994), this greater resistance to angular acceleration, coupled with the greater resistance to translational acceleration (due to relatively large limb masses), likely reduces primates' cursorial abilities.

Conclusions

The convergence of forelimb and hindlimb NPPs in the *Papio* sample provides some clues for the evolution of primate limb shapes. In order to preserve mobile and prehensile hands and feet, primates would have needed to maintain relatively distal CMs and RGs in their limbs. More cursorial mammals have followed a different evolutionary route by concentrating limb mass proximally to enhance their abilities to accelerate (Grand, 1977). Even though there are major differences in limb mass distribution between this sample of primates and the sample of *Canis* from Myers and Steudel (1997), their mechanisms for NPP convergence are similar. Both *Canis* and the *Papio* sample described above have relatively more distal mass in their forelimbs. This mass distribution pattern allows their shorter forelimbs to have relatively larger NPPs than their longer hindlimbs, and creates NPP convergence.

The impact of limb mass distribution pattern on primate locomotion may be great. The increased limb NPPs may lead to lower stride frequencies and longer stride lengths. These kinematic features of gait, which have been shown to be effective in not only on arboreal substrates, but on thin flexible branches, may have originally evolved as a byproduct of limb muscle adaptations for grasping hands and feet.

Acknowledgements

I would like to thank the Southwest Foundation for Biomedical Research for providing access to animals and for their generous help during data

collection. I would also like to thank Liza Shapiro, John Kappelman, Adam Gordon, Robert Scott, and three anonymous reviewers for their helpful suggestions on previous versions of this manuscript. Finally, I would like to thank Laura Alport for her help during data collection and Fredric Raichlen for help in developing the geometric model used in this study.

Appendix A. Calculation of segment inertial properties

As noted in the text, a and b describe the lengths of the major and minor axes of the elliptical column segment model and are given by second order polynomials of the form:

$$a=ez^2+dz+c \tag{A1}$$

$$b=kz^2+gz+f \tag{A2}$$

The mass can then be calculated by solving the definite integral:

$$Mass=\rho\int_0^l \pi abdz \tag{A3}$$

Where πab is the area of an ellipse, ρ is the density of the segment, and l is the length of the segment. Substituting Eq. (A1) and Eq. (A2) into Eq. (A3) and solving the definite integral gives the following equation for segment mass:

$$Mass=\rho\pi\left(cfz+\frac{1}{2}(df+cg)z^2+\frac{1}{5}ekz^5+\frac{1}{3}(ef+dg+ck)z^3+\frac{1}{4}(eg+dk)z^4\right) \tag{A4}$$

The center of mass can be found by solving the definite integral:

$$CM=\frac{\int_0^l \pi abzdz}{\int_0^l \pi abdz} \tag{A5}$$

Where the denominator in Eq. (A5) is the total mass of the segment. Substituting Eq. (A1) and Eq. (A2) into Eq. (A5) and solving the definite integral gives the following equation for segment CM:

$$CM=\frac{\left(\frac{1}{2}cfz^2+\frac{1}{3}(df+cg)z^3+\frac{1}{6}ekz^6+\frac{1}{4}(ef+dg+ck)z^4+\frac{1}{5}(eg+dk)z^5\right)}{\left(\frac{1}{5}ekz^5+cfz+\frac{1}{2}(df+cg)z^2+\frac{1}{3}(ef+dg+ck)z^3+\frac{1}{4}(eg+dk)z^4\right)} \tag{A6}$$

Eq. (A6) gives the position of the center of mass from the distal end. Subtracting this value from the segment length will give the position of the CM. from the proximal end. Finding the moment of inertia of the segment requires the use of a double integral of the form:

$$I=2\rho\int_0^l\int_{-a}^{a}(x^2+z^2)dAdz \tag{A7}$$

Where dA is an area element of the form:

$$dA=2y^*dx \tag{A8}$$

Where y is from the equation for an ellipse:

$$1=\frac{x^2}{a^2}+\frac{y^2}{b^2} \tag{A9}$$

Manipulating Eq. (A9) to solve for y gives:

$$y^2=\left(1-\frac{x^2}{a^2}\right)b^2 \tag{A10}$$

Taking the square root of both sides of Eq. (A10) gives:

$$y=b\sqrt{1-\frac{x^2}{a^2}} \tag{A11}$$

Substituting Eq. (A11) into Eq. (A8) gives the equation for dA:

$$dA = 2b\sqrt{1-\frac{x^2}{a^2}}\,dx \tag{A12}$$

Substituting Eq. (A12) into Eq. (A7) gives the equation for the mass moment of inertia.

$$I = 2\rho\int_0^l\int_{-a}^{a}(x^2+z^2)b\sqrt{1-\frac{x^2}{a^2}}\,dx\,dz \tag{A13}$$

Expanding Eq. (A13) gives:

$$I = 2\rho\int_0^l\int_{-a}^{a}\left(\frac{b}{a}x^2\sqrt{a^2-x^2}+\frac{b}{a}z^2\sqrt{a^2-x^2}\right)dx\,dz \tag{A14}$$

Integration of Eq. (A14) while holding z constant gives:

$$I = 2\rho\int_0^l\left(\frac{ba^3}{8}\pi+\frac{ba}{2}\pi z^2\right)dz \tag{A15}$$

Finally, substituting Eq. (A1) and Eq. (A2) into equation Eq. (A15) and solving the definite integral gives the following:

$$\begin{aligned}I = 2\rho\Big(&\frac{1}{2}\pi\Big(\frac{1}{3}cfz^3+\frac{1}{4}(df+cg)z^4+\frac{1}{7}ekz^7+\frac{1}{5}(ef+dg\\&+ck)z^5+\frac{1}{6}(eg+dk)z^6\Big)+\\&\Big(\frac{1}{8}\pi(c^3fz+\frac{1}{2}c^2(3df+cg)z^2+\frac{1}{9}e^3kz^9+\frac{1}{3}cz^3(3d^2f\\&+3cef+3cdg+c^2k)+\\&\frac{1}{8}e^2z^8(eg+3dk)+\frac{1}{4}z^4(d^3f+6cdef+3cd^2g+3egc^2\\&+3dkc^2)+\\&\frac{1}{7}ez^7(e^2f+3deg+3d^2k+3cek)+\frac{1}{6}z^6(3de^2f+3d^2eg\\&+3cge^2+d^3k+6cdek)+\\&\frac{1}{5}z^5(3d^2ef+3cfe^2+d^3g+6cdeg+3cd^2k+3c^2ek))))\end{aligned} \tag{A16}$$

Eq. (A16) gives the moment of inertia about the distal end of the segment. To find the moment of inertia about the segment CM, the parallel axis theorem (Eq. (A17)) must be applied.

$$I_{CM} = I-(mass)(CM)^2 \tag{A17}$$

References

Alexander, R.M., Jayes, A.S., Maloiy, G.M.O., Wathuta, E.M., 1981. Allometry of the leg muscles of mammals. J. Zool., Lond. 194, 539–552.

Alexander, R.M., Jayes, A.S., 1983. A dynamic similarity hypothesis for the gaits of quadrupedal mammals. J. Zool., Lond. 201, 135–152.

Alexander, R.M., Maloiy, G.M.O., 1984. Stride lengths and stride frequencies of primates. J. Zool., Lond. 202, 577–582.

Arshavski, Y.I., Kots, Y.M., Orlovskii, G.N., Rodinov, I.M., Shik, M.L., 1965. Investigations of the biomechanics of running by the dog. Biophysics 10, 737–746.

Basmajian, J.V., 1978. Muscle Alive. Their Functions Revealed by Electromyography. Williams and Wilkins, Baltimore.

Biewener, A.A., 1983. Allometry of quadrupedal locomotion: the scaling of duty factor, bone curvature and limb orientation to body size. J. Exp. Biol. 105, 147–171.

Cartmill, M., 1972. Arboreal adaptations and the origin of the order primates. In: Tuttle, R. (Ed.), The Functional and Evolutionary Biology of Primates. Aldine/Atherton, Chicago, pp. 97–102.

Cartmill, M., 1992. New views on primate origins. Evol. Anthrop. 1, 105–111.

Crompton, R.H., Li, Y., Alexander, R.M., Wang, W., Gunther, M.M., 1996. Segment inertial properties of primates: New techniques for laboratory and field studies of locomotion. Am. J. Phys. Anthrop. 99, 547–570.

Demes, B., Jungers, W.L., Nieschalk, U., 1990. Size- and speed-related aspects of quadrupedal walking in slender and slow lorises. In: Jouffroy, F.K., Stack, M.H., Niemitz, C. (Eds.), Gravity, Posture and Locomotion in Primates. Il Sedicesimo, Firenze, pp. 175–197.

English, A.W., 1978a. Functional analysis of the shoulder girdle of cats during locomotion. J. Morphol. 156, 279–292.

English, A.W., 1978b. An electromyographic analysis of forelimb muscles during overground stepping in the cat. J. Exp. Biol. 76, 105–122.

Fleagle, J.G., 1977. Locomotor behavior and muscular anatomy of sympatric Malaysian leaf monkeys (*Presbytis obscura* and *Presbytis melalophos*). Am. J. Phys. Anthrop. 46, 297–308.

Fleagle, J.G., 1988. Primate Adaptation and Evolution. Academic Press, San Diego.

Goslow, G.E. Jr, Seeherman, H.J., Taylor, C.R., McCutchin, M.N., Heglund, N.C., 1981. Electrical activity and relative length changes of dog limb muscles as a function of speed and gait. J. Exp. Biol. 94, 15–42.

Grand, T.I., 1977. Body weight: Its relation to tissue composition, segment distribution, and motor function. I. Interspecific comparisons. Am. J. Phys. Anthrop. 47, 211–240.

Hamrick, M.W., Rosenman, B.A., Brush, J.A., 1999. Phalangeal morphology of the paromomyidae (?Primates, Plesiadapiformes): the evidence for gliding behavior reconsidered. Am. J. Phys. Anthrop. 109, 397–413.

Hamrick, M.W., 2001. Primate origins: Evolutionary change in digital ray patterning and segmentation. J. Hum. Evol. 40, 339–351.

Heglund, N.C., 1985. Comparative energetics and mechanics of locomotion: How do primates fit in? In: Jungers, W.L. (Ed.), Size and Scaling in Primate Biology. Plenum Press, New York, pp. 319–335.

Hildebrand, M., 1985. Walking and running. In: Hildebrand, M., Bramble, D.M., Liem, K.F., Wake, D.B. (Eds.), Functional Vertebrate Morphology. Harvard University Press, Cambridge, pp. 38–57.

Hildebrand, M., Hurley, J.P., 1985. Energy of the oscillating legs of a fast-moving cheetah, pronghorn, jackrabbit and elephant. J. Morphol. 184, 23–31.

Hof, A.L., 1996. Scaling gait data to body size. Gait & Posture 4, 222–223.

Holt, K.G., Hamill, J., Andres, R.O., 1990. The force-driven harmonic oscillator as a model for human locomotion. Hum. Movement Sci. 9, 55–68.

Inman, V.T., Ralston, H.J., Todd, B., 1981. Human Walking. Williams and Wilkins, Baltimore, pp. 62–77.

Jungers, W.L., Stern, J.T., 1983. Body proportions, skeletal allometry and locomotion in the Hadar hominids: a reply to Wolpoff. J. Hum. Evol. 12, 673–684.

Larson, S.G., 1998. Unique aspects of quadrupedal locomotion in nonhuman primates. In: Strasser, E., Fleagle, J. (Eds.), Primate Locomotion. Plenum Press, New York, pp. 157–173.

Larson, S.G., Stern, J.T., 1989. The role of propulsive muscles of the shoulder during quadrupedalism in vervet monkeys (*Cercopithecus aethiops*): Implications for neural control of locomotion in primates. J. Motor Behav. 21, 457–472.

Larson, S.G., Schmitt, D., Lemelin, P., Hamrick, M., 2000. Uniqueness of primate forelimb posture during quadrupedal locomotion. Am. J. Phys. Anthrop. 112, 87–101.

Larson, S.G., Schmitt, D., Lemelin, P., Hamrick, M., 2001. Limb excursion during quadrupedal walking: how do primates compare to other mammals? J. Zool., Lond. 255, 353–365.

Lemelin, P., 1999. Morphological correlates of substrate use in didelphid marsupials: implications for primate origins. J. Zool. 247, 165–175.

Lemelin, P., Grafton, B., 1998. Grasping performance in *Saguinus midas* and the evolution of hand prehensility in primates. In: Strasser, E., Fleagle, J. (Eds.), Primate Locomotion. Plenum Press, New York, pp. 131–144.

Martin, P.E., 1985. Mechanical and physiological responses to lower extremity loading during running. Med. Sci. Sport Exer. 17, 427–433.

Mattes, S.J., Martin, P.E., Royer, T.D., 2000. Walking symmetry and energy cost in persons with unilateral tanstibial amputations: Matching prosthetic and intact inertial properties. Arch. Phys. Med. Rahabil. 81, 561–568.

Mochon, S., McMahon, T.A., 1980. Ballistic walking: an improved model. Math. Biosci. 52, 241–260.

Myers, M.J., Steudel, K., 1997. Morphological conservation of limb Natural Pendular Period in the domestic dog (*Canis familiaris*): Implications for locomotor energetics. J. Morphol. 234, 183–196.

Preuschoft, H., Gunther, M.M., 1994. Biomechanics and body shape in primates compared with horses. Z. Morph. Anthrop. 80, 149–165.

Reynolds, H.M., 1974. Measurement of the inertial properties of the segmented savannah baboon. PhD dissertation, Southern Methodist University.

Reynolds, T.R., 1987. Stride length and its determinants in humans, early hominids, primates, and mammals. Am. J. Phys. Anthrop. 72, 101–115.

Rosenblum, L.D., Turvey, M.T., 1988. Maintenance tendency in co-ordinated rythmic movements: relative fluctuations and phase. Neuroscience 27, 289–300.

Schmitt, D., 2003. Substrate size and primate forelimb mechanics: Implications for understanding the evolution of primate locomotion. Int. J. Primatol. 24, 1023–1036.

Schmitt, D., Larson, S.G., Stern, J.T. Jr, 1994. Serratus ventralis function in vervet monkeys: Are primate quadrupeds unique? J. Zool. 323, 215–230.

Selles, R.W., Bussmann, B.J., Wagenaar, R.C., Stam, H.J., 2001. Comparing predictive validity of four ballistic swing phase models of human walking. J. Biomech. 34, 1171–1177.

Skinner, H.B., Barrack, R.L., 1990. Ankle weighting effect on gait in able-bodied adults. Arch. Phys. Med. Rehab. 71, 112–115.

Steudel, K., 1990. The work and energetic cost of locomotion: I. The effects of limb mass distribution in quadrupeds. J. Exp. Biol. 154, 273–285.

Steudel-Numbers, K.L., 2003. The energetic cost of locomotion: humans and primates compared to generalized endotherms. J. Hum. Evol. 44, 255–262.

Taylor, C.R., Heglund, N.C., Maloiy, G.M.O., 1982. Energetics and mechanics of terrestrial locomotion: I. Metabolic energy consumption as a function of speed and body size in birds and mammals. J. Exp. Biol. 97, 1–21.

Tipler, P.A., 1976. Physics. Worth, New York.

Turvey, M.T., Schmidt, R.C., Rosenblum, L.D., 1988. On the time allometry of co-ordinated rhythmic movements. J. theoret. Biol. 130, 285–325.

Vilensky, J.A., 1979. Masses, centers-of-gravity, and moments-of-inertia of the body segments of the Rhesus monkey (*Macaca mulatta*). Am. J. Phys. Anthrop. 50, 57–65.

Vilensky, J.A., Gankiewicz, E., Townsend, D.W., 1988. Effects of size on vervet (*Cercopithecus aethiops*) gait parameters: A cross-sectional approach. Am. J. Phys. Anthrop. 76, 463–480.

Vilensky, J.A., Gankiewicz, E., 1990a. Effects of speed on forelimb joint angular displacement patterns in vervet monkeys (*Cercopithecus aethops*). Am. J. Phys. Anthrop. 83, 203–210.

Vilensky, J.A., Gankiewicz, E., 1990b. Effects of growth and speed on hindlimb joint angular displacement patterns in vervet monkeys (*Cercopithecus aethops*). Am. J. Phys. Anthrop. 81, 441–449.

Wells, J.P., DeMenthon, D.F., 1987. Measurements of the body segment mass, center of gravity, and determination of moments of inertia by double pendulum in *Lemur fulvus*. Am. J. Primatol. 12, 299–308.

Whitehead, P.F., Larson, S.G., 1994. Shoulder motion during quadrupedal walking in *Cercopithecus aethiops*: Integration of cineradiographic and electromyographic data. J. Hum. Evol. 26, 525–544.

Whittlesey, S.N., van Emmerick, R.E.A., Hamill, J., 2000. The swing phase of human walking is not a passive movement. Motor Control 4, 273–292.

Witte, H., Preuschoft, H., Recknagel, S., 1991. Human body proportions explained on the basis of biomechanical principles. Z. Morph. Anthrop. 78, 407–423.